RSC Advances

PAPER

View Article Online
View Journal | View Issue

Cite this: *RSC Adv.*, 2016, **6**, 40706

Chemical components from the seeds of *Catalpa bungei* and their inhibitions of soluble epoxide hydrolase, cholinesterase and nuclear factor kappa B activities†

Hao-Yu Tang,[a] Meng-Meng Bai,[a] Jun-Mian Tian,[a] Gennaro Pescitelli,[b] Trpimir Ivšić,[bc] Xiao-Hua Huang,*[a] Hyunwoo Lee,[d] Ya Nan Son,[d] Jang Hoon Kim,[d] Young Ho Kim[d] and Jin-Ming Gao*[a]

Received 16th February 2016
Accepted 18th April 2016

DOI: 10.1039/c6ra04207d

www.rsc.org/advances

Two new chlorinated iridoids, named bungosides A (**1**) and B (**2**), were isolated from the seeds of *Catalpa bungei* (family Bignoniaceae). Their structures were elucidated on the basis of NMR analysis. Twenty known compounds (**3–22**) were also characterized, including in one case (6-*O*-*p*-hydroxybenzoylglutinoside, **3**) the assignment of the absolute configuration by employing electronic circular dichroism (CD) and time-dependent density functional theory (TDDFT) calculations. Compounds **1–3** were unusual cage-like iridoids with an oxygen bridge between C-3 and C-10. Among the isolates, ursolic acid lactone (**14**) was the most active soluble epoxide hydrolase (sEH) inhibitor with an IC_{50} 19.1 ± 0.8 μM. In addition, D-pinoresinol (**19**) and ladanein (**21**) displayed selectively inhibitory effects on butyrylcholinesterase (BChE) with IC_{50} of 31.5 ± 0.4 μM and 33.0 ± 2.3 μM, respectively, but not acetylcholinesterase (AChE) activity, and only compound **18** suppressed NF-κB activity in HepG2 cells (IC_{50} 21.53 ± 2.37 μM).

Introduction

Soluble epoxide hydrolase (sEH) is an important bifunctional enzyme with potent biological activities on vascular and renal systems. It can hydrolyze epoxyeicosatrienoic acids (EETs), metabolites of arachidonic acid generated by epoxygenase CYP enzymes, into dihydroxyeicosatrienoic acids (DHETs).[1] The former produce significant biological effects in vascular and renal systems while the latter don't show much beneficial function. EETs are endothelium-derived hyperpolarizing factors (EDHFs) which act as regulators of vascular function.[2] The cardiovascular effects of EETs include vasodilation, anti-migratory actions on vascular smooth muscle cells and anti-inflammatory action.[1] Therefore, the inhibition of sEH becomes an effective pathway to treat cardiovascular disease. Alzheimer's disease (AD) is one of the most common neurodegenerative diseases in elderly population. Reduced synthesis of the neurotransmitter acetylcholine is thought to be a main cause of AD.[3] Therefore, cholinesterase inhibitors became an important cognitive enhancing treatment based on the facts that they could increase the content of acetylcholine at cholinergic synapses. Both acetylcholinesterase (AChE) and butyrylcholinesterase (BChE) participate in hydrolyzing brain acetylcholine in different manners.[4] AChE and BChE have thus been the main targets to prevent AD.

Inflammation contributes to the pathogenesis of cancer, cardiovascular diseases, and type-2 diabetes mellitus.[5] The nuclear factor kappaB (NF-κB) is a key regulator of many pro-inflammatory pathways.[5] NF-κB normally resides in the cytoplasm, where it is retained by association with the endogenous inhibitor of kappa B (IκB) protein.[6] However, when activated by inflammatory stimuli such as tumor necrosis factor alpha (TNF-α), injury, or other stress-related stimuli, NF-κB is released, translocates to the nucleus and binds to DNA resulting in the transcription of proinflammatory target genes.[7] Therefore, inhibitors targeting NF-κB signaling are considered as potential candidates for both prevention and therapy of inflammation.

The *Catalpa* plants of Bignoniaceae family include about 13 species in the world and are mainly distributed in America and East Asia. Previous phytochemical investigation indicated that

[a]*Shaanxi Key Laboratory of Natural Products & Chemical Biology, College of Science, Northwest A&F University, Yangling 712100, P. R. China. E-mail: jinminggao@nwsuaf.edu.cn; x.h.huang@163.com; Tel: +86-29-87092515*

[b]*Dipartimento di Chimica e Chimica Industriale, Università di Pisa, via Moruzzi 3, I-56124 Pisa, Italy*

[c]*Division of Organic Chemistry and Biochemistry, Ruđer Bošković Institute, 10000 Zagreb, Croatia*

[d]*College of Pharmacy, Chungnam National University, Daejeon 305-764, Republic of Korea*

† Electronic supplementary information (ESI) available: HR-ESI-MS, NMR, and IR spectra of compounds **1–3**, bioactive data of compounds. See DOI: 10.1039/c6ra04207d

Catalpa plants contain iridoids and naphthoquinones as the main constituents with various pharmacological properties such as antifungal, cytotoxic, antitumor, and antiplasmodial activities.[8–11] *Catalpa bungei* C. A. Mey is widely distributed in China, and the fruits of the tree have been used in folk medicine for edema, nephritis, cystitis, eczema, leprosy and gastric cancer.[12] However, few secondary metabolites from the seeds of this plant have been reported.

In continuation of our investigation on the bioactive constituents from traditional Chinese medicines in the Qinba Mountains,[13–16] we carried out chemical investigations on the seeds of *C. bungei* and evaluated their sEH, AChE and BChE inhibitory activities. In this study, two new compounds (**1**, **2**), along with 20 known natural compounds that belong to various groups of iridoids, triterpenoids, phenylethanoid glycosides, and lignans, were isolated from the seeds of *C. bungei*. Their inhibitions of sEH, AChE and BChE were also assessed. Herein, we report the isolation and structural elucidation of the new compounds (**1**, **2**), as well as enzymatic inhibitory activity of these compounds. The present study could lay a foundation for the medicinal development of *C. bungei*.

Results and discussion

The EtOAc-soluble fraction of a 75% EtOH extract of seeds of *C. bungei*, was chromatographed by means of different chromatographic techniques using normal-phase silica gel, reversed-phase C18 gel, Sephadex LH-20 and RP-HPLC to afford three new (**1** and **2**) and 20 known compounds (Fig. 1).

The identification of the known compounds, des-*p*-hydroxybenzoyl kisasagenol B (**4**),[11] rehmaglutin C (**5**),[17] des-*p*-hydroxybenzoyl-3-deoxycatalpin (**6**),[18] 6-*O*-(*p*-hydroxybenzoyl)-D-glucopyranose (**7**),[19] 6-*O*-[(*E*)-feruloyl]-D-glucopyranose (**8**),[20] 6-*O*-*p*-coumaroyl-D-glucopyranose (**9**),[21] ursolic acid (**10**),[22] rotundic acid (**11**),[23] arjunic acid (**12**),[24] 2α,3α,19α-trihydroxy-12-oleanen-28-oic acid (**13**),[25] ursolic acid lactone (**14**),[26] martynoside (**15**),[27] verbascoside (kusaginin or acteoside, **16**),[28] balanophonin (**17**),[29] 9α-hydroxysesamin (**18**),[30] D-pinoresinol (**19**),[31] 9-methoxy-α-lapachone (**20**),[32] ladanein (**21**),[33] and *p*-hydroxybenzoic acid (**22**),[34] was confirmed by comparing their physical and spectroscopic data with those reported in the literature. The known compounds included various types of iridoids, triterpenoids, phenylethanoid glycosides, and lignans. To the best of our knowledge, compounds **1–22** (except **3**) were isolated from *C. bungei* for the first time, of which **7–9**, **11–14**, and **17–19**, in particular the occurrence of ursane and oleanane triterpenes, were first isolated from the genus of *Catalpa*.

Compound **3** was obtained as a white powder. The molecular formula was established as $C_{22}H_{27}ClO_{12}$ by HR-ESI-MS at *m*/*z* 541.1081 $[M + Na]^+$, indicating nine degrees of unsaturation. Its IR spectrum indicated the presence of hydroxy (3400 cm^{-1}), conjugated carbonyl ester (1693 cm^{-1}), and aromatic (1607 and 1514 cm^{-1}) functionalities in the molecule. The ^{13}C NMR and DEPT data (Table 1) exhibited 22 signals, including three methylenes, fifteen methines, and four quaternary carbons. The ^1H and ^{13}C NMR spectroscopic data suggested the presence of two acetal groups (δ_H 5.70, δ_C 93.1 and δ_H 5.36, δ_C 95.9), one tertiary hydroxyl group (δ_C 79.9), one oxymethylene (δ_H 4.09 and 3.72, δ_C 62.1), an aromatic unit, and a β-glucopyranosyl moiety. These assignments were further confirmed by the HMBC correlations forming the cyclopentanopyrane ring skeleton, a *p*-hydroxybenzoyl and a β-glucopyranosyl residue. The ^1H NMR spectrum (Table 1) showed the presence of a doublet signal at δ_H 5.70 (J = 2.1 Hz, 1H) that is a characteristic signal for H-1 of an iridoid.[35] The ^{13}C signals at δ_C 98.9, 74.2, 78.1, 71.6, 78.1, and 62.7 in the ^{13}C NMR spectrum were characteristic for a β-D-glucopyranosyl residue. The β-configuration for the glucose was supported from the large coupling constant (J = 8.0 Hz) for the anomeric doublet signal at δ_H 4.73 (H-1′). HMBC correlations of δ_H 5.70 (H-1) and δ_C 98.9 (C-1′), and δ_H 4.73 (H-1′) and δ_C 93.1 (C-1) indicated that the glucopyranosyl unit was attached to C-1 of the aglycone. The chemical shift of C-7 at δ_C 70.4 indicated that the Cl atom was located at C-7.[36,37] Detailed interpretation of the ^1H and ^{13}C NMR spectral data (Table 1) indicated that **3** contains a *p*-hydroxybenzoyl group [δ_H 7.92 (d, J = 8.8 Hz, H-2″,6″), 6.87 (d, J = 8.8 Hz, H-3″,5″); δ_C 168.6 (C-7″), 164.3 (C-4″), 121.4 (C-1″)]. The attachment of the *p*-hydroxybenzoyl unit on C-6 (δ_C 87.9) of the aglycone was established from the HMBC correlation between H-6 at δ_H 5.13 and the ester carbonyl carbon (δ_C 168.6) of the *p*-hydroxybenzoyl group (Fig. 2).

The relative stereochemistry at C-1, C-5, and C-9 was determined to be the same as found in other iridoid glucosides based on the small coupling of $J_{1,9}$ (2.1 Hz) and the large coupling of $J_{5,9}$ (9.8 Hz). The configuration of the 8-OH was confirmed to be β from the C-9 chemical shift (δ_C 48.3), which is a characteristic of assignment of the configuration of the 8-OH.[38] This β-configuration causes the deshielding of C-9 in comparison to its α counterpart in the following pairs of C-8 isomers, 10-des-cinnamoylglobularimin and 10-des-cinnamoylglobularinin,[39] and gardenoside and monotropein methyl ester.[38] The configuration of the H-3 proton was determined to be β on the basis of the formation of the intramolecular acetal of C-3 with the C-10 OH.[40] As a result, compound **3** was elucidated as a rigid tricyclic iridoid. Similar iridoids possessing a cage-like skeleton have been isolated from *Picrorhiza kurroa*,[41] *Catalpa bignonioides*,[42] and *Rehmannia glutinosa*[43] and also obtained through bromination and dehydration of the catalposide extracted from the roots of *Picrorhiza kurroa*.[44]

Compound **3** is a derivative of glutinoside, which was isolated previously from the dried root of *Rehmannia glutinosa*.[45] It had not been isolated previously as a pure natural form but as a semi-synthetic hexaacetate, obtained through acetylation of crude extract of *Catalpa* species.[11] Here, the NMR data of **3** are reported for the first time. The structure of this compound was confirmed by detailed analysis of the 2D-NMR data (HSQC, HMBC, ^1H–^1H COSY, and NOESY spectra) (Fig. 2). On the basis of the above analysis, the structure of **3** was determined to be 6-*O*-*p*-hydroxybenzoylglutinoside. In order to further determine the structure of **3**, we prepare its hexaacetate (**3a**), whose NMR data are in good agreement with published data.[11] Since the absolute configuration of the hexaacetate of **3** was not directly determined in the original paper,[11] we decided to assign it independently by means of electronic circular dichroism (CD) spectroscopy. The experimental UV absorption and CD

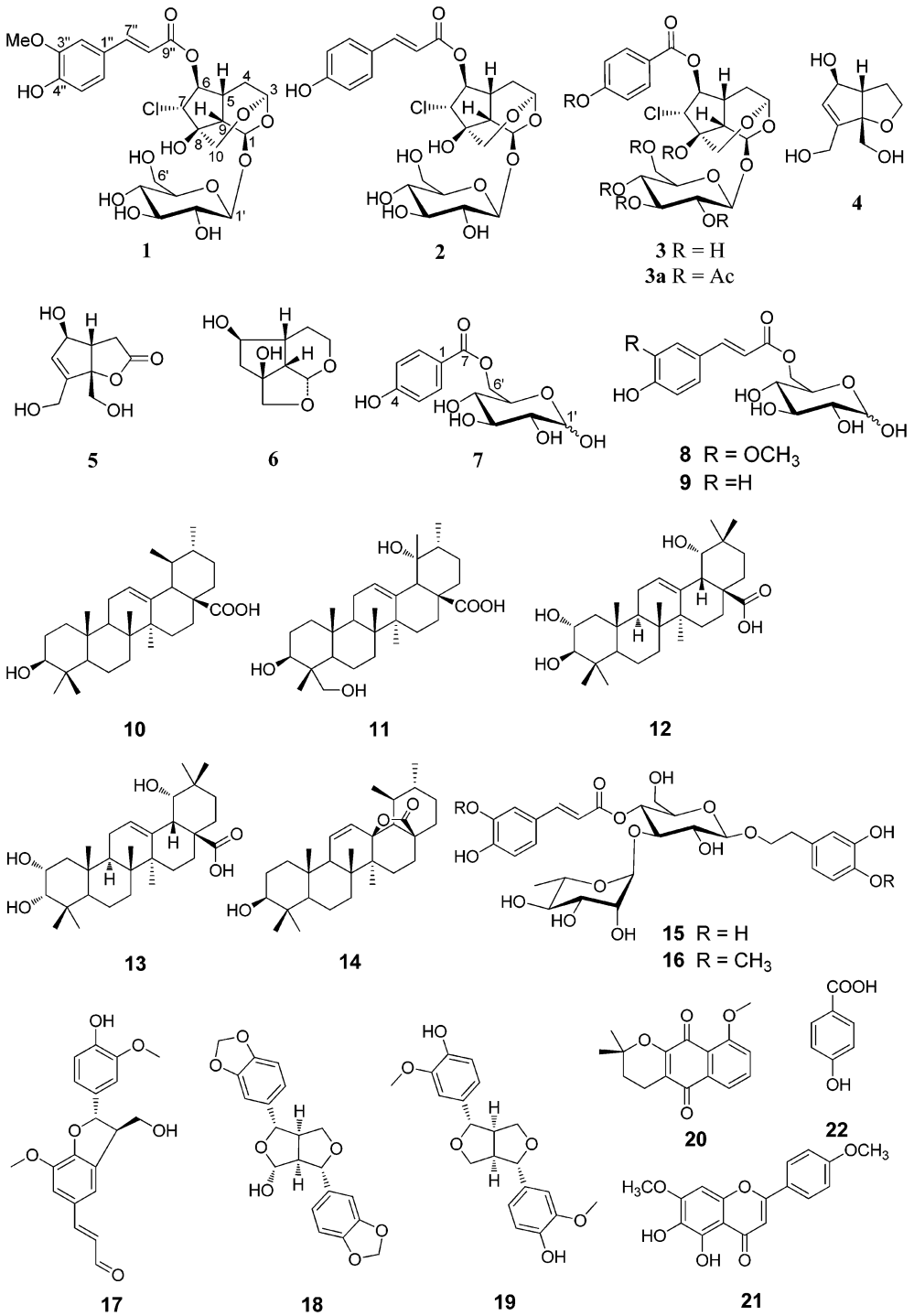

Fig. 1 Structures of isolated compounds **1–22** from *C. bungei*.

spectrum of (−)-**3** in acetonitrile are reported in Fig. 3. The UV consists of two main bands mainly associated with the electronic transitions of the *p*-hydroxy benzoate chromophore. Correspondingly, the CD spectrum shows three major bands above 220 nm and a positive tail at shorter wavelengths. To simulate the CD spectrum by TDDFT calculations,[46] we first generated a set of structures reproducing low-energy conformers in solution, using a well-established procedure based on a Monte Carlo conformational search followed by geometry optimizations with DFT method. The resulting set of conformations was composed by two main families, one devoid of any intramolecular hydrogen bond, and one showing consistently an intramolecular hydrogen bond between glucose 6′-OH and the ester carbonyl group. Such a hydrogen bond leads to the formation of a 14-membered cycle which is quite disfavored by entropic factors, and it is likely to be a computational

Table 1 NMR spectroscopic data of compounds **1–3** (in MeOH-d_4)

	1		**2**		**3**	
No.	δ_C	δ_H (multi. J in Hz)	δ_C	δ_H (multi. J in Hz)	δ_C	δ_H (multi. J in Hz)
1	93.1 d	5.70 d, 2.1	93.1 d	5.64 d, 2.0	93.1 d	5.70 d, 2.1
3	95.9 d	5.35 d, 3.0	95.9 d	5.30 d, 2.9	95.9 d	5.36 d, 3.0
4	34.4 t	2.49 dd, 13.7, 8.3; 2.13 dd, 13.7, 3.0	34.4 t	2.43 dd, 13.6, 8.5; 2.07 dd, 13.6, 2.9	34.4 t	2.49 dd, 13.5, 8.5; 2.16 dd, 13.5, 3.0
5	34.8 d	2.40, m	34.7 d	2.34 m	34.7 d	2.43, m
6	87.7 d	5.05 dd, 8.3, 2.7	87.7 d	4.99 dd, 8.3, 2.7	87.9 d	5.13 dd, 8.3, 2.7
7	70.4 d	4.46 d, 8.3	70.4 d	4.41 d, 8.1 Hz	70.4 d	4.54 dd, 8.3, 0.9
8	79.9 s		79.9 s		79.9 s	
9	48.3 d	2.65 d, 9.9	48.3 d	2.59 d, 9.9	48.3 d	2.67 d, 9.8
10	62.1 t	4.08 d, 11.9; 3.72 d, 11.9	62.1 t	4.02 d, 11.8; 3.65 m	62.1 t	4.09 dd, 12.2, 0.8; 3.72 d, 12.2
1′	99.0 d	4.73 d, 8.0	98.9 d	4.67 d, 8.3	98.9 d	4.73 d, 8.0
2′	74.7 d	3.19 dd, 9.1, 8.0	74.7 d	3.14 t, 8.3	74.2 d	3.18 dd, 9.0, 8.0
3′	78.2 d	3.41, m	78.1 d	3.35, m	78.1 d	3.40, m
4′	71.6 d	3.31, m	71.6 d	3.26, m	71.6 d	3.31, m
5′	78.1 d	3.31, m	78.1 d	3.28, m	78.1 d	3.30, m
6′	62.7 t	3.70, m; 3.90, m	62.7 t	3.85, m; 3.65, m	62.7 t	3.70, m; 3.91, m
1″	127.6 s		127.0 s		121.4 s	
2″	111.9 s	7.25 d, 1.8	131.3 d	7.46 d, 8.6	132.9 d	7.92 d, 8.8
3″	149.4 s		116.9 d	6.79 d, 8.6	116.4 d	6.87 d, 8.8
4″	150.8 s		161.5 s		164.3 s	
5″	116.5 d	6.85 d, 8.2	116.9d	6.79 d, 8.6	116.4 d	6.87 d, 8.8
6″	124.3 d	7.13 dd, 8.2, 1.8	131.3 d	7.46 d, 8.6	132.9 d	7.92 d, 8.8
7″	147.5 d	7.68 d, 15.9	147.2 d	7.62 d, 15.8	168.6 s	
8″	114.9 d	6.45 d, 15.9	114.5 d	6.36 d, 15.9		
9″	168.8 s		168.9 s			
OCH_3	56.5 q	3.93, s				

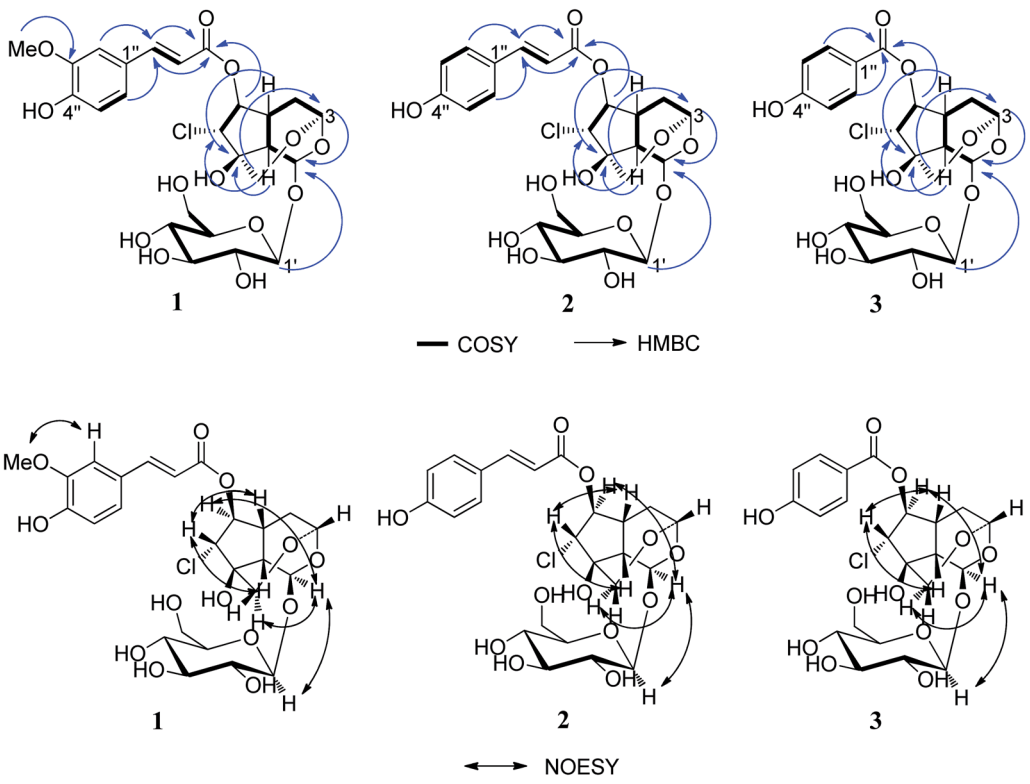

Fig. 2 Selected HMBC, COSY and NOESY correlations for **1–3**.

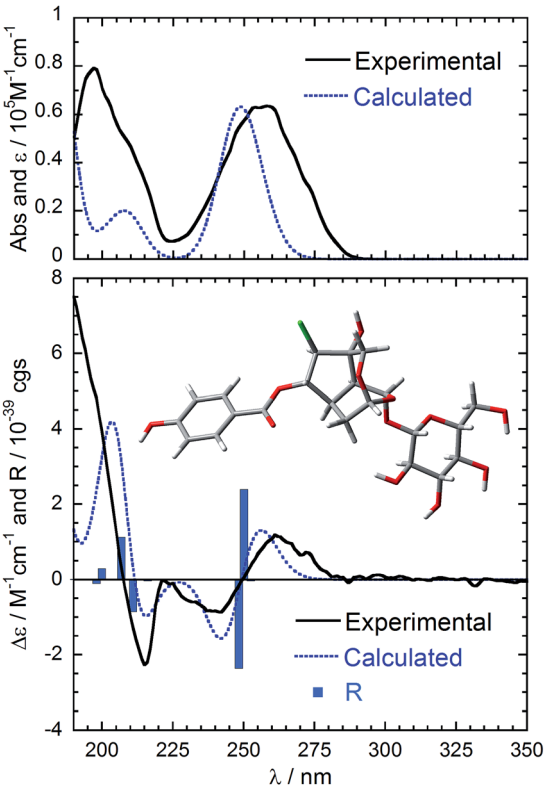

Fig. 3 Experimental UV absorption and CD spectra of compound (−)-**3** compared with TDDFT-calculated spectra at B3LYP/TZVP level on B3LYP/6-31G(d) geometries for (1*S*,3*R*,5*R*,6*S*,7*R*,8*S*,9*S*)-**3**, as Boltzmann average at 300 K for all structures with population >1%. Experimental spectra: concentration 0.54 mM in acetonitrile; cell path-length 0.05 cm. Calculated spectra: Gaussian band-shape with 0.2 eV exponential half-width; scaled by a factor 3; no shift applied. Vertical bars represent computed rotational strengths. Inset: lowest-energy DFT conformer of compound (1*S*,3*R*,5*R*,6*S*,7*R*,8*S*,9*S*)-**3** showing no 6′-OH···O=C intramolecular hydrogen bond.

artifact.[47] In fact, the NOESY spectrum of **3** did not show any cross-peak expected for such a cyclic structure, *e.g.* between H-2″ and CH_2-6′. Therefore, we neglected these hydrogen-bonded conformers from our set; however we also checked that the inclusion of hydrogen-bonded conformers in TDDFT calculations would not affect the final assignment (results not shown). As a consequence, we obtained a restricted set of low-energy conformers including 9 structures with relative energies within 1.8 kcal mol^{-1} and populations >1% at room temperature; the lowest-energy conformer is shown in the inset in Fig. 3. All 9 conformers share the same conformation of the polycyclic skeleton, which seems to be very rigid, and also the same conformation of the *p*-hydroxy benzoate group, defining a dihedral angle (O=)C–O–C-6–H-6 around −40°. The 9 structures differ only in the flip of 4″-OH and in the rotamerism of the glucose OH groups. Accordingly, the CD spectra calculated with TDDFT method at B3LYP/TZVP level for the whole conformational set were similar to each other. The Boltzmann-weighted average of the spectra is shown in Fig. 3. The CD spectrum calculated for enantiomer (1*S*,3*R*,5*R*,6*S*,7*R*,8*S*,9*S*)-**3** is in very good agreement with the experimental CD spectrum measured for (−)-**3**. Therefore, we may assign 6-*O*-*p*-hydroxybenzoyl glutinoside the absolute configuration (−)-(1*S*,3*R*,5*R*,6*S*,7*R*,8*S*,9*S*). Not surprisingly, this is the same configuration reported for the analogs of glutinoside,[45] 6-*O*-*p*-hydroxybenzoyl asystasioside E[11] and piscroside A,[48] all of which are ultimately related to rehmaglutin D.[49]

Compound **1** was obtained as a white powder. The molecular formula $C_{25}H_{31}ClO_{13}$ was established by HR-ESI-MS at *m*/*z* 597.1343 $[M + Na]^+$, requiring 10 degrees of unsaturation. Its IR spectrum indicated the presence of hydroxy (3393 cm^{-1}) and α,β-unsaturated ester carbonyl (1697 cm^{-1}) groups, and an aromatic moiety (1598, 1516 cm^{-1}) in the molecule. The ^{13}C NMR and DEPT data (Table 1) showed the presence of one methyl, three methylenes, sixteen methines, and five quaternary carbons. The presence of a sugar moiety was evidenced by a set of signals observed in the ^1H NMR spectrum between δ_H 4.73 and 3.19, and signals observed in the ^{13}C NMR spectrum (Table 1) at δ_C 62.7, 71.6, 74.7, 78.1, 78.2, and 99.0. The coupling constant of the anomeric proton at δ_H 4.73 (d, J = 8.0 Hz, H-1′) indicated the β-configuration of the glucopyranose. Acid hydrolysis afforded D-glucose based on GC analysis.

Detailed interpretation of the ^1H and ^{13}C NMR spectral data (Table 1) indicated that the chemical structure of compound **1** was very similar to those of 6-*O*-*p*-hydroxybenzoylglutinoside (**3**), except for the presence of an (*E*)-*p*-feruloyl group [δ_H 7.25 (d, J = 1.8 Hz, H-2″), 7.13 (dd, J = 8.2, 1.9 Hz, H-6″), 6.85 (d, J = 8.2 Hz, H-5″), 7.68 (d, J = 15.9 Hz, H-7″), 6.45 (d, J = 15.9 Hz, H-8″); δ_C 168.8 (C-9″), 127.6 (C-1″)] in **1**. The location of the feruloyl group at C-6 (δ_C 87.7) was supported by the correlation of H-6 (δ_H 5.05, dd, J = 8.3, 2.7 Hz) to the ester carbonyl at C-9″ (δ_C 168.8) in the HMBC spectrum (Fig. 2). The HMBC correlations of the H-1 acetal signal at δ_H 5.70 (d, J = 2.1 Hz) to the C-1′ anomeric carbon at δ_C 99.0 and the C-3 acetal carbon at δ_C 95.9 indicated that the glucose residue was attached to C-1 of the aglycon, which was further linked to C-3 through an ether linkage. In addition, on the basis of the downfield shift of C-10 (δ_C 62.1) and HMBC correlation from H_2-10 (δ_H 4.08, 3.72) to C-3 (δ_C 95.9), the acetal carbon C-3 was determined to be linked to C-10 through an oxo bridge. The methine carbon at δ_C 70.4 was assigned to C-7, attached to one chlorine atom,[36,37] which was confirmed from the HMBC correlation of H_2-10 to C-7 and from HR-ESI-MS data.

The relative configuration of **1** was confirmed by a NOESY experiment (Fig. 2) as well as from biosynthetic considerations. According to molecular modeling of this compound, the oxo bridge from C-3 to C-10 could only be α-oriented, and the 8-OH and H-9 could only be β-oriented. In the NOESY spectrum, the correlations between H-7 and H-5β, H-7 and H-9β, and H-6 and H-1α indicated that H-7 and H-6 were in β- and α-orientation, respectively, thereby establishing the stereochemistry of the Cl and the feruloyl group as α and β, respectively. In addition, the chemical-shift as well as coupling-constant values of the iridoid moiety of **1** (Table 1) were very similar to those reported for compound **3**, suggesting that **1** possesses the same configuration (−)-(1*S*,3*R*,5*R*,6*S*,7*R*,8*S*,9*S*) as **3**. The structure of this compound was confirmed by detailed analysis of the 2D-NMR data including its HSQC, HMBC, ^1H–^1H COSY, and NOESY

spectra (Fig. S5–S8 and Table S1 in the ESI†). Consequently, the structure of **1** was determined to be 6-*O*-feruloylglutinoside, named bungoside A.

Compound **2** was assigned a molecular formula of $C_{24}H_{29}ClO_{12}$, as established by the HR-ESI-MS at *m*/*z* 567.1243 $[M + Na]^+$. The IR, UV, and NMR spectroscopic data (Table 1) of **2** closely resembled those of **1**, except that the C-6 substituent group in **2** is a (*E*)-*p*-coumaroyl group [δ_H 7.46 (2H, d, J = 8.6 Hz, H-2″,6″), 6.79 (2H, d, J = 8.6 Hz, H-3″,5″), 7.62 (1H, d, J = 15.9 Hz, H-7″), 6.36 (1H, d, J = 15.9 Hz, H-8″); δ_C 168.9 (C-9″), 127.0 (C-1″)] instead of an (*E*)-feruloyl group. This was supported by the correlation of H-6 at δ_H 4.99 (dd, J = 8.3, 2.7 Hz) to the ester carbonyl at C-9″ (δ_C 168.9) in the HMBC spectrum. The structure of this compound was confirmed by detailed analysis of the 2D-NMR data including its HSQC, HMBC, ^{1}H–^{1}H COSY, and NOESY spectra (Fig. S14–S17 and Table S2 in the ESI†). ROESY correlations suggested the same relative configuration as **1** and **3**. Similarly, compound **2** was suggested to possess the same absolute configuration (−)-(1*S*,3*R*,5*R*,6*S*,7*R*,8*S*,9*S*) due to the same sign of specific rotation as **3** and **1** as well as to their same biogenetic relationships. Consequently, the structure of **2** was established to be (−)-(1*S*,3*R*,5*R*,6*S*,7*R*,8*S*,9*S*)-6-*O*-(*E*)-*p*-coumaroylglutinoside, named bungoside B.

The compounds **1–22** (except **9**) were tested for their inhibitory effects on soluble epoxide hydrolase,[16] acetylcholinesterase (AChE) and butyrylcholinesterase (BChE) at 100 μM (Table S4†). Compounds **1**, **8**, **10**, **14**, **15**, **17** and **20** showed inhibitory rate over 50% on sEH. Their IC_{50} values were determined in the following work (Table 2). Among the seven compounds tested, **14** showed the most active inhibitory activity on sEH with an IC_{50} value of 19.1 ± 0.8 μM; other compounds exhibited weak activity with IC_{50} values of 30–50 μM. In addition, kinetic curve of **14** on sEH showed it inhibits sEH by a mixed mode with inhibition constant K_i value 7.9 ± 1.7 μM (Fig. 4). Compounds **19** and **21** were found to display satisfactory inhibitory effects on AChE and BChE. Then only components **19** and **21** were tested their IC_{50} values on the two enzymes, and the results are observed in Table 2. Compounds **19** and **21** displayed selectively moderate inhibitory effects on butyrylcholinesterase (BChE) with IC_{50} values of 31.5 ± 0.4 μM and 33.0 ± 2.3 μM, respectively, but not acetylcholinesterase (AChE) activity. Moreover, kinetic curve of **19** and **21** on BChE (Table 2) showed they inhibited this enzyme by a mixed mode with K_i values of 7.8 ± 0.3 and 11.3 ± 2.9 μM, respectively (Fig. 5). To the best of our knowledge, this is the first report on **14** as sEH inhibitor as well as on the inhibition of **21** on BChE.

Furthermore, compounds **1–22** (except **9**) were assessed for their effects on TNFα-induced NF-κB transcriptional activity in human hepatocarcinoma (HepG2) cells using an NF-κB-luciferase assay. As shown in Table 2, among the tested compounds, only compound **18** significantly inhibited TNFα-induced NF-κB transcriptional activity with IC_{50} values of 21.53 ± 2.37 μM, while others were weak little or inactive. Apigenin (IC_{50} 1.64 μM) was used as a positive control. To date, there is no

Table 2 sEH, AChE, BChE and NF-κB inhibitory activities of compounds

compd[a]	sEH inhibitory activity IC_{50}[a,c] (μM)	AChE inhibitory activity IC_{50}[c,d] (μM)	BChE inhibitory activity IC_{50}[c,d] (μM)	NF-κB inhibitory activity IC_{50}[c,d] (μM)
1	50.4 ± 2.0	NT[e]	NT	ND
2	NT	NT	NT	>100
3	NT	NT	NT	52.78 ± 2.26
4	NT	NT	NT	>100
5	NT	NT	NT	ND
6	NT	NT	NT	ND
7	NT	NT	NT	ND
8	44.6 ± 3.4	NT	NT	>100
9	—	NT	—	—
10	36.6 ± 7.7	NT	NT	33.93 ± 2.53
11	NT	NT	NT	>100
12	NT	NT	NT	96.4 ± 2.35
13	NT	NT	NT	98.0 ± 2.36
14	19.1 ± 0.8	NT	NT	32.88 ± 2.46
15	30.6 ± 2.0	NT	NT	46.91 ± 2.74
16	NT	NT	NT	>100
17	53.8 ± 1.2	NT	NT	ND
18	NT	NT	NT	21.53 ± 2.37
19	NT	NT	31.59 ± 0.44	>100
20	37.0 ± 1.4	NT	NT	31.64 ± 2.20
21	NT	86.36 ± 0.93	33.09 ± 2.34	52.4 ± 2.25
22	NT	NT	NT	>100
AUDA[b]	10.9 ± 1.2 nM	—	—	—
Tacrine[b]	—	207.84 ± 4.29 nM	7.46 ± 0.86 nM	—
Apigenin[b]	—	—	—	1.64 ± 0.19

[a] All compounds were examined in a set of experiments three times. [b] Positive control. [c] Statistical significance was determined by one-way analysis of variance followed by Dunnett's multiple comparison test, $P < 0.05$ *versus* control. [d] Data were expressed as mean ± SD of at least three experiments performed in triplicate. [e] NT not tested.

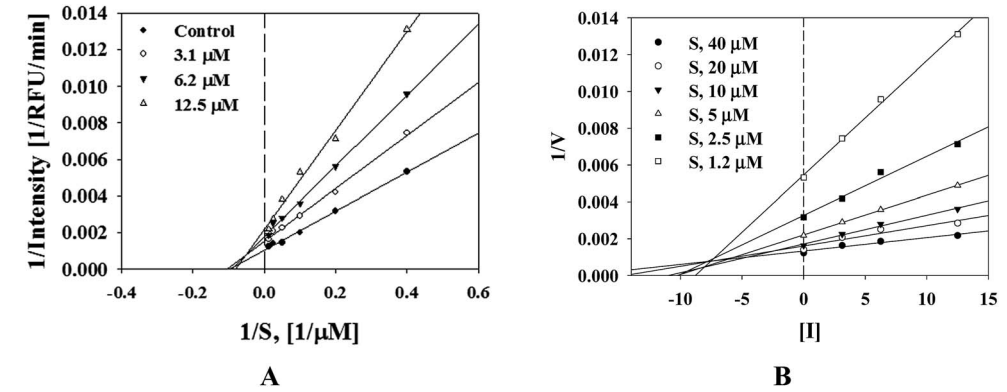

Fig. 4 Lineweaver–Burk plot for the sEH inhibition of compound **14** (A). Dixon plot of sEH inhibition by **14** (B).

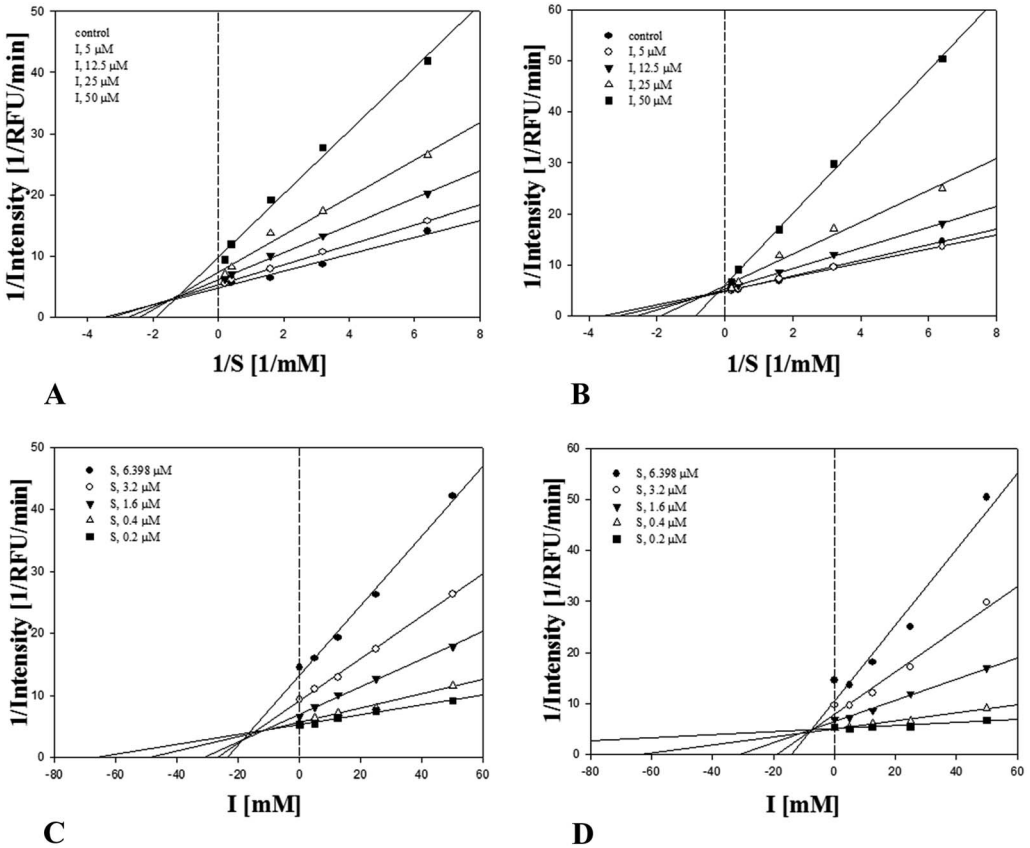

Fig. 5 Lineweaver–Burk plot for BChE inhibition of compounds **19** (A) and **21** (B); Dixon plot of BChE inhibition by **19** (C) and **21** (D).

literature on the anti-inflammatory effects of compound **18**. These results led us to conclude that ursolic acid lactone (**14**) and 9α-hydroxysesamin (**18**) from the seeds of *Catalpa bungei* exhibit significant anti-inflammatory effects by inhibition of sEH enzyme and TNFα-induced NF-κB activation, and that D-pinoresinol (**19**) and ladanein (**21**) inhibit BChE. These results also provide scientific support for the use of *Catalpa bungei* in the prevention of cancer, inflammatory and neurodegenerative diseases.

In conclusion, three cage-like chlorinated iridoid glucosides (**1–3**) including two new bungoside A (**1**) and bungoside B (**2**), as well as 19 compounds, were isolated from the seeds of *Catalpa bungei*. Among the isolates, ursolic acid lactone (**14**) showed a potential inhibitory activity against soluble epoxide hydrolase (sEH), and 9α-hydroxysesamin (**18**) significantly inhibited TNFα-induced NF-κB transcriptional activity. Furthermore, D-pinoresinol (**19**) and ladanein (**21**) displayed marked inhibitory effects on BChE. Our observations provide scientific support for the use of *Catalpa bungei* in the prevention of cancer, inflammatory and neurodegenerative diseases.

Experimental

General experimental procedures

Optical rotations were measured with a DKSH Automatic A21101 polarimeter. UV spectra were obtained using a Thermo Scientific Evolution 300 UV-VIS Spectrophotometer. ^{1}H and ^{13}C NMR spectra were recorded on 400 MHz and 500 MHz NMR instruments (Bruker Daltonics Inc., Bremen, Germany). Chemical shifts were reported using solvent residual peak as the internal standard. ESI-MS spectra were performed on a Thermo Fisher LTQ Fleet instrument spectrometer (Thermo Fisher Scientific Inc., MA, U.S.). Column chromatography (CC) was performed on silica gel (90–150 μm) (Qingdao Marine Chemical Inc., Qingdao, China), Sephadex LH-20 (40–70 μm) (Amersham Pharmacia Biotech AB, Uppsala, Sweden), and Lichroprep RP-18 gel (40–63 μm; Merck, Darmstadt, Germany). GF_{254} plates (Qingdao Marine Chemical Inc., Qingdao, China) were used for thin-layer chromatography (TLC). Preparative TLC (PTLC) was carried out on silica gel 60 GF_{254} (Qingdao Marine Chemical, Ltd., Qingdao, China); semi-preparative HPLC (Waters Corp., Milford) was performed by a Thermo BDS Hypersil column (250 × 4.6 mm and 250 × 10 mm, 5 μm) (Thermo Fisher Scientific Inc., MA).

Reagents. 3-Phenyl-cyano(6-methoxy-2-naphthalenyl)methyl ester-2-oxiraneacetic acid (PHOME), 12-[[(tricyclo[3.3.1.13,7] dec-1-ylamino)carbonyl]amino]-dodecanoic acid (AUDA), and purified recombinant sEH were purchased from Cayman (Cayman, Michigan). The other chemical reagents and standard compounds were purchased from Sigma-Aldrich (St. Louis, MO). AB-8 macroporous resin was purchased from the Chemical Plant of Nankai University (Tianjin, China), which was cross-linked polystyrene copolymer. All used chemicals (methanol, chloroform, ethyl acetate, petroleum ether and *n*-butanol *etc.*) were purchased from Kelong Chemical Engineering (Kelong, Chengdu, China). HPLC methanol was purchased from Tedia company (Tedia Inc., Fairfield, Connecticut). Ultrapure water was made in our lab.

Acetylcholinesterase (AChE) from electric eel (Type-VI-S, E.C. 3.1.1.7), acetylthiocholine iodide (ATChI), butyrylcholinesterase (BChE) from equine serum (E.C. 3.1.1.8), butyrylthiocholine iodide (BTChI), 5,5′-dithiobis(2-nitrobenzoic acid) (DTNB), tacrine were obtained from Sigma-Aldrich (St. Louis, MO). Potassium phosphate were purchased from Amresco (K_2HPO_4) and Daejung (KH_2PO_4).

Plant materials

The seeds of *Catalpa bungei* C. A. Mey were collected from Lveyang County, Shaanxi Province of China on November 25, 2012. The plant was taxonomically identified by one of authors (K. J. Z.). A voucher specimen (LXY-01239) has been deposited at the Herbarium of College of Life Sciences, Northwest A&F University, P. R. China.

Extraction and isolation

The dried and powdered seeds (20 kg) of *C. bungei* were extracted three times with 75% EtOH at room temperature. The solvent was evaporated under reduced pressure to obtain a crude EtOH extract (1.042 g), which was suspended in H_2O and partitioned successively with petroleum ether (PE), EtOAc, and *n*-BuOH. The EtOAc fraction (*ca.* 250 g) was chromatographed on silica gel over CC eluting with EtOAc/MeOH (20 : 1, 15 : 1, 10 : 1, 7 : 1, 5 : 1) to give five fractions 1–5. Fraction 4 (16 g) was subjected to silica gel CC using $CHCl_3$/MeOH (10 : 1–2 : 1) to give four fractions 4.1–4.4. Fraction 4.1 was fractionated on Sephadex LH-20 with MeOH and then further purified by a silica gel column using PE/acetone (7 : 1) to afford **10** (17 mg). Fraction 4.2 was loaded to silica gel CC using $CHCl_3$/MeOH (5 : 1–2 : 1) as eluent to give four fractions (4.2.1–4.2.4). Fraction 4.2.2 was purified by RP-18 CC using MeOH/H_2O (0 : 10–5 : 5) as a solvent to give **4** (88 mg) and **15** (27 mg). Fraction 4.2.3 was rechromatographed over RP-18 column (30% methanol) and further purified by RP-HPLC using MeOH/H_2O (25 : 75, flow rate: 3 mL min^{-1}) to afford **1** (18.5 mg, $t_R = 37.5$ min) and **2** (17.1 mg, $t_R = 42.5$ min).

Fraction 4.3 was separated by CC over RP-18 with 10–50% MeOH. Subfraction eluted with 50% MeOH was purified by silica gel CC eluting with $CHCl_3$/MeOH (5 : 1), followed by semi-preparative RP-HPLC using MeOH/H_2O (40 : 60; flow rate = 2 mL min^{-1}) to obtain **3** (30 mg, $t_R = 18.5$ min).

Fraction 4.4 was separated by a Sephadex LH-20 column and then RP-18 CC. Its water fraction was purified on CC over silica gel with $CHCl_3$/MeOH (5 : 1) as eluent to give **5** (9 mg).

Fraction 1 was applied to a silica gel column by elution with EtOAc/MeOH (20 : 1–5 : 1) to generate three fractions (1.1–1.3). Fraction 1.1 was loaded to medium pressure liquid chromatography over RP-C18 by gradient elution with MeOH/H_2O (40–100%) to furnish 6 fractions (1.1.1–1.1.6). Fraction 1.1.1 eluted by 40% MeOH was purified by Sephadex LH-20 to give **22** (90 mg). Fraction 1.1.2 (eluted by 50% MeOH) was purified by Sephadex LH-20 and then by CC over silica gel and eluted by $CHCl_3$/MeOH (10 : 1) to obtain **17** (14.5 mg). Fraction 1.1.3 was separated successively by Sephadex LH-20, RP-18 CC (45% MeOH) and then silica gel CC ($CHCl_3$/MeOH 5 : 1) to give **20** (6.5 mg). Fraction 1.1.4 was submitted to Sephadex LH-20 to furnish three fractions (1.1.4.1–1.1.4.3). Fraction 1.1.4.1 was purified by CC on silica gel eluting with $CHCl_3$/MeOH (7 : 1) to give **18** (20.0 mg). Fraction 1.1.4.2 was purified by CC on silica gel and further Sephadex LH-20 to provide **19** (9.0 mg). Fraction 1.1.4.3 was recrystallized to give **21** (20 mg) in MeOH. Fraction 1.1.5 (80% MeOH) was separated successively by CC over Sephadex LH-20, RP-18, and silica gel ($CHCl_3$/MeOH 50 : 1) to produce **12** (11.6 mg) and **13** (6.7 mg). Fraction 1.1.6 was purified successively by Sephadex LH-20, RP-18 (85% MeOH), and CC on silica gel ($CHCl_3$/MeOH 20 : 1) to afforded **14** (7.0 mg).

Fraction 1.2 was fractionated successively by CC over silica gel, Sephadex LH-20, and RP-18 (70% MeOH) and then by silica gel CC ($CHCl_3$/MeOH 25 : 1) to give **11** (9.3 mg). Fraction 3 was separated by reduced pressure CC over RP-18 eluting by using MeOH/H_2O in a gradient elution (from 1 : 10 to 5 : 5) to yield six fractions (3.1–3.6). Fraction 3.1 was separated by Sephadex LH-20 and silica gel CC using $CHCl_3$/MeOH (20 : 1) to give **6** (9 mg). Fraction 3.2 was separated by Sephadex LH-20 to furnish two fractions (3.2.1–3.2.2). Fraction 3.2.1 was purified by semi-

preparative RP-HPLC using MeOH/H_2O (40 : 60; flow rate: 3 mL min^{-1}) to give **9** (5.5 mg, $t_R = 18.5$ min) and **8** (13.5 mg, $t_R = 19.3$ min). Compound **7** (15.1 mg) was isolated from fraction 3.2.2 by using silica gel CC eluted with $CHCl_3$/MeOH (8.5 : 1), and compound **16** (181 mg) was obtained from fraction 3.3 using Sephadex LH-20 and silica gel CC eluting with $CHCl_3$/MeOH/H_2O (4 : 1 : 0.02).

The purity of every purified chemicals was more than 98% by HPLC.

Bungoside A (1). White powder; $[\alpha]_D^{21}$ – 15.7 (*c* 0.17, MeOH); UV (MeOH) λ_{max} (log ε) 328 nm (4.28); IR (KBr) ν_{max} 3393, 1697, 1630, 1598, 1516 cm^{-1}; ^1H and ^{13}C NMR data, see Table 1. ESI-MS (positive) *m*/*z* 597.49 $[M + Na]^+$; HR-ESI-MS *m*/*z* 597.1343 ($[M + Na]^+$, calcd $C_{25}H_{31}ClO_{13}Na^+$, 597.1351).

Bungoside B (2). White powder; $[\alpha]_D^{20}$ – 14.3 (*c* 0.12, MeOH); UV (MeOH) λ_{max} (log ε) 316 nm (4.23); IR (KBr) ν_{max} 3383, 1690, 1631, 1604, 1514 cm^{-1}; ^1H and ^{13}C NMR data, see Table 1. ESI-MS (positive) *m*/*z* 567.23 $[M + Na]^+$; HR-ESI-MS *m*/*z* 567.1243 ($[M + Na]^+$, calcd $C_{24}H_{29}ClO_{12}Na^+$, 567.1245).

6-*O*-*p*-Hydroxybenzoylglutinoside (3). White powder; $[\alpha]_D^{21}$ – 19.5 (*c* 0.11, MeOH); UV (MeOH) λ_{max} (log ε) 261 nm (4.37); IR (KBr) ν_{max} 3400, 1693, 1607, 1514 cm^{-1}; ^1H and ^{13}C NMR data, see Table 1. ESI-MS (positive) *m*/*z* 541.38 $[M + Na]^+$; HR-ESI-MS *m*/*z* 541.1081 ($[M + Na]^+$, calcd $C_{22}H_{27}ClO_{12}Na^+$, 541.1089).

Acetylation of 3

Compound **3** (3 mg) was treated with acetic anhydride (0.2 mL) in dry pyridine (0.2 mL) at room temperature. The mixture was stirred for 24 h, on workup to give a pure derivative **3a** (*ca.* 3 mg).

2′,3′,4′,6′,4″,8-*O*-Hexaacetoyl-6-*O*-*p*-hydroxybenzoylglutinoside (3a). White powder; $C_{34}H_{39}ClO_{18}$; ESI-MS *m*/*z* 793.25 $[M + Na]^+$; ^{13}C NMR (125 MHz, $CDCl_3$) δ 170.8 (C–$\underline{C}OCH_3$), 170.4 (C–$\underline{C}OCH_3$), 167.0 (C–$\underline{C}OCH_3$), 169.5 (C–$\underline{C}OCH_3$), 169.21 (C–$\underline{C}OCH_3$), 168.9 (C–$\underline{C}OCH_3$), 165.7 (C-11), 154.8 (C-15), 131.6 (C-13,17), 127.0 (C-12), 121.9 (C-14, 16), 95.3 (C-1′), 94.5 (C-1), 91.9 (C-3), 86.2 (C-6), 85.9 (C-8), 72.9 (C-3′), 72.2 (C-5′), 71.04 (C-2′), 68.3 (C-4′), 63.0 (C-7), 61.7 (C-6′), 60.0 (C-10), 42.0 (C-9), 33.5 (C-5), 32.9 (C-4), 22.3 (C–CO$\underline{C}H_3$), 21.3 (C–CO$\underline{C}H_3$), 20.9 (C–CO$\underline{C}H_3$), 20.8 (C–CO$\underline{C}H_3$), 20.7 (C-2 × CO$\underline{C}H_3$); ^1H NMR (500 MHz, $CDCl_3$) δ 8.08 (2H, d, J = 8.7 Hz, H-13, 17), 7.20 (2H, d, J = 8.7 Hz, H-14,16), 5.58 (1H, d, J = 2.0 Hz, H-1), 5.49 (1H, d, J = 8.0 Hz, H-7), 5.39 (1H, d, J = 2.7 Hz, H-3), 5.22 (1H, ddd, J = 9.4, 7.3, 2.2 Hz, 3′), 5.17 (1H, dd, J = 8.0, 2.8 Hz, H-6), 5.11 (1H, t, J = 9.7 Hz, H-4′), 4.96 (2H, m, H-1′,2′), 4.31 (2H, m, H-6′b,10α), 4.15 (1H, dd, J = 12.4, 2.3 Hz, H-6′a), 3.90 (1H, d, J = 12.5 Hz, H-10β), 3.73 (1H, ddd, J = 10.0, 4.1, 2.4 Hz, H-5′), 3.60 (1H, br d, J = 10.3 Hz, H-9), 2.40 (1H, m, H-5), 2.33 (3H, s, H–CO$\underline{CH}_3$), 2.29 (1H, m, H-4β), 2.11, 2.10, 2.02, 2.01, 1.99 (each 3H, s, H–CO$\underline{CH}_3$), 2.06 (1H, m, H-4α).

Acid hydrolysis of 1–3 and determination of sugar

Compounds **1–3** (2.0 mg, each) was hydrolysed with 2 M HCl–dioxane (1 : 1, 1 mL) at 100 °C for 2 h. The reaction mixture was partitioned between chloroform and H_2O three times. The aqueous layer was neutralized with 2 M Ag_2CO_3 and evaporated *in vacuo*. The residue was dissolved in pyridine (0.5 mL), to which L-cysteine methyl ester hydrochloride in pyridine (0.1 M, 0.5 mL) was added. After reacting at 60 °C for 1 h, trimethylsilylimidazole (0.05 mL) was added to the reaction mixture and kept at 4 °C for another 8 h. The mixture was analysed by GC-MS. By comparison of the retention time of the authentic sample, the monosaccharide of compounds **1–3** was determined to be D-glucose (t_R = 11.85 min) (t_R = 12.15 min of L-glucose).

Biological assays

sEH inhibition activity assay. The inhibition of sEH was assayed using a hydrolysis reaction of PHOME in the presence of the sEH enzyme.[16] Briefly, 130 μL of sEH (62.5 ng mL^{-1}) in 25 mM bis–Tris buffer (including 0.1% bovine serum albumin, pH 7.0) and 20 μL of ligands diluted in MeOH were mixed in 96 well plate. 50 μL of PHOME (40 μM) in buffer was added as substrate. After starting the sEH reaction at 37 °C, products were measured using a Genios microplate reader (Tecan, Mannedorf, Switzerland) during an hour at excitation and emission wavelengths of 320 and 465 nm, respectively. sEH inhibitory activity for each sample was calculated as follows:

$$\text{sEH inhibitory activity (\%)} = 100 - [(S_{60} - S_0)/(C_{60} - C_0)] \times 100$$

where C_{60} and S_{60} were the fluorescence of control and inhibitor after 60 min, S_0 and C_0 is the fluorescence of control and inhibitor at zero min.

Cholinesterase inhibition assay. The AChE and BChE inhibitory activity measurements were performed according to the literature protocol.[50] In brief, 0.1 M potassium buffer (pH 7.4), 130 μL of 0.05 U mL^{-1} AChE and BChE, 20 μL of tested compound (1 mM) were mixed and pre-incubated for 30 min at 25 °C. The reaction was then initiated with the addition of 25 μL of 5 mM ATChI and BTChI, 25 μL of 1 mM DTNB. AChE and BChE activity was determined spectrophotometrically through measuring the change in ultraviolet absorbance of an assay solution at 405 nm over a period of 15 min at 37 °C. Tacrine (3.8–500 nM) was used as positive control.

NF-κB inhibitory activity assay.[16] The luciferase vector was first transfected into human hepatocarcinoma HepG2 cells. After a limited amount of time, the cells were lysed, and luciferin, the substrate of luciferase, was introduced into the cellular extract along with Mg^{2+} and an excess of ATP. Under these conditions, luciferase enzymes expressed by the reporter vector could catalyze the oxidative carboxylation of luciferin. Cells were seeded at 2×10^5 cells per well in 12-well plates and grown. After 24 h, cells were transfected with inducible NF-κB luciferase reporter and constitutively expressing Renilla reporter. After 24 h of transfection, medium was changed to assay medium (Opti-MEM + 0.5% FBS + 0.1 mM NEAA + 1 mM sodium pyruvate + 100 units per mL penicillin + 10 μg mL^{-1} streptomycin) and cells were pretreated for 1 h with either vehicle (DMSO) and compounds, followed by 1 h of treatment with 10 ng mL^{-1} TNF-α for 20 h. Unstimulated cells were used as a negative control (−), apigenin was used as a positive control. Dual luciferase assay was performed 48 h after transfection, and

promoter activity values are expressed as arbitrary units using a Renilla reporter for internal normalization.

Computational section

MMFF and DFT calculations were run with Spartan'14 (Wavefunction, Inc., Irvine CA, 2014), with standard parameters and convergence criteria. TDDFT calculations were run with Gaussian'09,[51] with default grids and convergence criteria. Conformational searches were run with the Monte Carlo algorithm implemented in Spartan'14 using Merck molecular force field (MMFF). All structures thus obtained were optimized with DFT method using B3LYP functional and 6-31G(d) basis set *in vacuo*. TDDFT calculations were run using B3LYP functional and TZVP basis set, including 24 excited states. On some selected structures, other functionals (CAM-B3LYP, PBE0, M06, M06-2X) and basis sets (augmented TZVP, ADZP) were also tested, leading to consistent results. UV and CD spectra were generated using the program SpecDis.[52] by applying a Gaussian band shape with 0.2 eV exponential half-width, from dipole-length rotational strengths.

Acknowledgements

This work was financially supported by the National Forestry Public Welfare Industry Research Project (201204603) and the Program of Science & Technology of Shaanxi Province (2013SF2-15) as well as by the Priority Research Center Program (2009-0093815) through the National Research Foundation of Korea (NRF) funded by the Ministry of Education, Science and Technology, Republic of Korea. T. I. gratefully acknowledges FP7-REGPOT-2012-2013-1, grant agreement number 316289–InnoMol.

Notes and references

1 J. D. Imig and B. D. Hammock, *Nat. Rev. Drug Discovery*, 2009, **8**, 794–805.
2 W. B. Campbell, D. Gebremedhin, P. F. Pratt and D. R. Harder, *Circ. Res.*, 1996, **78**, 415–423.
3 P. T. Francis, A. M. Palmer, M. Snape and G. K. Wilcock, *J. Neurol., Neurosurg. Psychiatry*, 1999, **66**, 137–147.
4 E. Giacobini, *Pharmacol. Res.*, 2004, **50**, 433–440.
5 L. Tornatore, A. K. Thotakura, J. Bennett, M. Moretti and G. Franzoso, *Trends Cell Biol.*, 2012, **22**, 557–566.
6 Z. H. Wu and S. Miyamoto, *J. Mol. Med.*, 2007, **85**, 1187–1202.
7 N. S. Rial, K. Choi, T. Nguyen, B. Snyder and M. J. Slepian, *Med. Hypotheses*, 2012, **78**, 29–32.
8 (*a*) E. Kanai, K. Machida and M. Kikuchi, *Chem. Pharm. Bull.*, 1996, **44**, 1607–1609; (*b*) A. Fujiwara, T. Mori, A. Iida, S. Ueda, Y. Hano, T. Nomura, H. Tokuda and H. Nishino, *J. Nat. Prod.*, 1998, **61**, 629–632; (*c*) K. Machida, E. Hishinuma and M. Kikuchi, *Chem. Pharm. Bull.*, 2004, **52**, 618–621; (*d*) J. Y. Cho, H. Y. Kim and G. J. Choi, *Pest Manage. Sci.*, 2006, **62**, 414–418.
9 J. H. Kuk, S. J. Ma, J. H. Moon, K. Y. Kim, S. H. Choi and K. H. Park, *J. Microbiol. Biotechnol.*, 2002, **12**, 858–863.
10 F. Dal Piaz, A. Vassallo, A. Temraz, R. Cotugno, M. A. Belisario, G. Bifulco, M. G. Chini, C. Pisano, N. De Tommasi and A. Braca, *J. Med. Chem.*, 2013, **56**, 1583–1595.
11 K. Machida, M. Ogawa and M. Kikuchi, *Chem. Pharm. Bull.*, 1998, **46**, 1056–1057.
12 W. T. Lee, *Coloured standard illustration of Korean plants*, Academy Publishing Co., 1996, p. 326.
13 J. J. Tang, F. Y. Zhang, D. M. Wang, J. M. Tian, S. Dong and J. M. Gao, *Int. J. Mol. Sci.*, 2013, **14**, 19484–19493.
14 H. W. Liu, X. Z. Yu, D. Padula, G. Pescitelli, Z. W. Lin, F. Wang, K. Ding, M. Lei and J. M. Gao, *Eur. J. Med. Chem.*, 2013, **59**, 265–273.
15 (*a*) D. M. Wang, C. C. Zhang, Q. Zhang, N. Shafiq, G. Pescitelli, D. W. Li and J. M. Gao, *J. Agric. Food Chem.*, 2014, **62**, 6669–6676; (*b*) J. M. Gao, W. J. Wu and J. W. Zhang, *Nat. Prod. Rep.*, 2007, **24**, 1153–1189.
16 (*a*) M. M. Bai, W. Shi, J. M. Tian, M. Lei, Y. H. Kim, Y. N. Sun, J. H. Kim and J. M. Gao, *J. Agric. Food Chem.*, 2015, **63**, 2198–2205; (*b*) H. Li, J. M. Tian, H. Y. Tang, S. Y. Pan, A. L. Zhang and J. M. Gao, *RSC Adv.*, 2015, **5**, 29185–29192.
17 C. A. Boros and F. R. Stermitz, *J. Nat. Prod.*, 1991, **54**, 1173–1246.
18 K. Machida, C. Ikeda, R. Kakuda, Y. Yaoita and M. Kikuchi, *Nat. Med.*, 2001, **55**, 61–63.
19 T. Kaneko, K. Ohtani, R. Kasai, K. Yamasaki and M. D. Nguyen, *Phytochemistry*, 1998, **47**, 259–263.
20 M. Wang, J. Li, M. Rangarajan, Y. Shao, E. J. LaVoie, T. C. Huang, C. T. Ho and J. Agric, *Food Chem.*, 1998, **46**, 4869–4873.
21 H. Shimomura, Y. Sashida and T. Adachi, *Phytochemistry*, 1988, **27**, 641–644.
22 S. X. Yang, J. M. Gao, J. C. Qin, L. Zhou, M. H. Chiu and L. Wang, *Helv. Chim. Acta*, 2007, **90**, 1477–1481.
23 F. P. Soares, C. A. V. Ronconi, E. V. L. da Cunha, J. M. Barbosa-Filho, M. S. da Silva and R. Braz-Filho, *Magn. Reson. Chem.*, 1998, **36**, 608–614.
24 B. K. Ponou, R. B. Teponno, M. Ricciutelli, T. B. Nguelefack, L. Quassinti, M. Bramucci, G. Lupidi, L. Barboni and L. A. Tapondjou, *Chem. Biodiversity*, 2011, **8**, 1301–1309.
25 T. H. Lee, S. S. Lee, Y. C. Kuo and C. H. Chou, *J. Nat. Prod.*, 2001, **64**, 865–869.
26 N. M. Al Musayeib, R. A. Mothana, A. A. Gamal, S. M. Al-Massarani and L. Maes, *Molecules*, 2013, **18**, 9207–9218.
27 T. Ersoz, D. Tasdemir, I. Calis and C. M. Ireland, *Turk. J. Chem.*, 2002, **26**, 465–471.
28 B. Gering and M. Wichtl, *J. Nat. Prod.*, 1987, **50**, 1048–1054.
29 S. H. Wu, Y. M. Shen, Y. W. Chen, Z. Y. Li, L. Y. Yang and S. L. Li, *Chem. Nat. Compd.*, 2009, **45**, 536–538.
30 A. L. Sousa, Q. S. Sales, R. Braz-Filho and R. R. de Oliveira, *J. Liq. Chromatogr. Relat. Technol.*, 2012, **35**, 2294–2303.
31 L. H. Xie, T. Akao, K. Hamasaki, T. Deyama and M. Hattori, *Chem. Pharm. Bull.*, 2003, **51**, 508–515.
32 H. Itokawa, K. Matsumoto, H. Morita and K. Takeya, *Phytochemistry*, 1992, **31**, 1061–1062.
33 M. H. Farjam, A. Rustaiyan, E. Ezzatzadeh and A. R. Jassbi, *Iran. J. Pharm. Res.*, 2013, **12**, 395–400.

34 A. Andolfi, A. Boari, M. Evidente, A. Cimmino, M. Vurro, G. Ash and A. Evidente, *J. Nat. Prod.*, 2015, **78**, 623–629.
35 C. A. Boros and F. R. Stermitz, *J. Nat. Prod.*, 1990, **53**, 1055–1147.
36 X. P. Yang, E. W. Li, Q. Zhang, C. S. Yuan and Z. J. Jia, *Chem. Biodiversity*, 2006, **3**, 762–770.
37 R. Wang, D. Xiao, Y. H. Bian, X. Y. Zhang, B. J. Li, L. S. Ding and S. L. Peng, *J. Nat. Prod.*, 2008, **71**, 1254–1257.
38 R. K. Chaudhuri, F. Ü. Afifi-Yazar and O. Sticher, *Helv. Chim. Acta*, 1979, **62**, 1603–1604.
39 R. K. Chaudhuri and O. Sticher, *Tetrahedron Lett.*, 1979, **34**, 3149–3152.
40 S. K. Ling, T. Tanaka and I. Kouno, *J. Nat. Prod.*, 2001, **64**, 796–798.
41 Q. Jia, M. F. Hong and D. Minter, *J. Nat. Prod.*, 1999, **62**, 901–903.
42 T. Iwagawa, T. Hamada, S. Kurogi, T. Hase, T. Okubo and M. Kim, *Phytochemistry*, 1991, **30**, 4057–4060.
43 M. Yoshikawa, Y. Fukuda, T. Taniyama and I. Kitagawa, *Chem. Pharm. Bull.*, 1986, **34**, 1403–1406.
44 K. Weinges, H. Schick, K. Neuberger, H. J. Ziegler, J. Lichtenthäler and H. Irngartinger, *Liebigs Ann. Chem.*, 1989, **11**, 1113–1122.
45 I. Kitagawa, Y. Fukuda, T. Taniyama and M. Yoshikawa, *Chem. Pharm. Bull.*, 1995, **43**, 1096–1100.
46 J. Autschbach, L. Nitsch-Velasquez and M. Rudolph, *Top. Curr. Chem.*, 2011, **298**, 1–98.
47 S. Iwahana, H. Iida, E. Yashima, G. Pescitelli, L. Di Bari, A. G. Petrovic and N. Berova, *Chem.–Eur. J.*, 2014, **20**, 4386–4395.
48 H. Wang, F. H. Wu, F. Xiong, J. J. Wu, L. Y. Zhang, W. C. Ye, P. Li and S. X. Zhao, *Chem. Pharm. Bull.*, 2006, **54**, 1144–1149.
49 I. Kitagawa, Y. Fukuda, T. Taniyama and M. Yoshikawa, *Chem. Pharm. Bull.*, 1991, **39**, 1171–1176.
50 G. L. Ellman, K. D. Courtney Jr., V. Andres, *et al.*, *Biochem. Pharmacol.*, 1961, **7**, 88–95.
51 M. J. Frisch, G. W. Trucks, H. B. Schlegel, G. E. Scuseria, M. A. Robb, J. R. Cheeseman, G. Scalmani, V. Barone, B. Mennucci, G. A. Petersson, H. Nakatsuji, M. Caricato, X. Li, H. P. Hratchian, A. F. Izmaylov, J. Bloino, G. Zheng, J. L. Sonnenberg, M. Hada, M. Ehara, K. Toyota, R. Fukuda, J. Hasegawa, M. Ishida, T. Nakajima, Y. Honda, O. Kitao, H. Nakai, T. Vreven, J. A. Montgomery Jr., J. E. Peralta, F. Ogliaro, M. Bearpark, J. J. Heyd, E. Brothers, K. N. Kudin, V. N. Staroverov, T. Keith, R. Kobayashi, J. Normand, K. Raghavachari, A. Rendell, J. C. Burant, S. S. Iyengar, J. Tomasi, M. Cossi, N. Rega, J. M. Millam, M. Klene, J. E. Knox, J. B. Cross, V. Bakken, C. Adamo, J. Jaramillo, R. Gomperts, R. E. Stratmann, O. Yazyev, A. J. Austin, R. Cammi, C. Pomelli, J. W. Ochterski, R. L. Martin, K. Morokuma, V. G. Zakrzewski, G. A. Voth, P. Salvador, J. J. Dannenberg, S. Dapprich, A. D. Daniels, O. Farkas, J. B. Foresman, J. V. Ortiz, J. Cioslowski and D. J. Fox. *Gaussian 09, Revision D.01*, Gaussian, Inc., Wallingford, CT, 2013.
52 T. Bruhn, A. Schaumlöffel, Y. Hemberger and G. Bringmann, *Chirality*, 2013, **25**, 243–249.